

# INDOOR LOCATION AWARENESS BASED ON THE NON-COHERENT CORRELATION FUNCTION FOR GNSS SIGNALS\*

*Danai Skournetou and Elena Simona Lohan*

Institute of Communications Engineering, Tampere University of Technology  
P.O.Box 553, FIN-33101, Finland;  
{danai.skournetou, elena-simona.lohan}@tut.fi

## ABSTRACT

In this paper we propose a novel Carrier-to-Noise Ratio (CNR) identifier for separating the indoor and outdoor regions in satellite-based navigation applications. This CNR identifier is based on the Level Crossing Rate (LCR) of the non-coherently averaged correlation function between the incoming signal and the reference code. The CNR identifier is tested in static and fading, single and multi-path channels for Galileo and GPS signals. We show that, using the proposed identifier, we are able to distinguish the indoor from outdoor scenarios in up to 80% – 95% of situations.

## 1. INTRODUCTION

The need for estimating the Carrier to Noise Ratio (CNR) is undoubtedly present in all types of communication channels. In particular, a priori information of signal's strength can be of great use when satellite communication is concerned, where numerous error sources (e.g. orbital errors, atmospheric effects, multipath, etc.) may affect the transmitted signal and consequently distort it.

Additionally, the growing demand for higher position accuracy requires successful error mitigation even in low CNR scenarios. This implies that CNR-adaptive signal processing methods could be of great potential in the context of Global Navigation Satellite Systems (GNSS). Moreover, the emerging need for indoor positioning requires "smart identifiers" of the environment for successful distinction between indoor and outdoor. Typical CNR estimators for GNSS signals are based on the first and higher-order moments of the complex envelope of the received signal (e.g., second-order and fourth-order moments) [1, 2, 3] and they require rather heavy computations at the receiver. Also, a CNR estimator based on combined wideband and narrowband samples has been proposed in [4]. However, this estimator seems to

work only at CNR levels above 40 dB/Hz and has a rather high complexity [2].

To summarize the above discussion, the CNR estimators for GNSS signals are still rather scarce in the literature. The goal of our paper is to introduce a novel indoor/outdoor identifier, based on the Level Crossing Rate (LCR), which is built from the non-coherent averaged Absolute value of the correlation function (Acf). By difference with the previous estimators, our identifier is an on-off CNR estimator, meaning that it tries to distinguish the low signal levels from the high signal levels, with the purpose of differentiating between indoor and outdoor scenarios. The typical indoor and outdoor CNR levels will be discussed in Section 2.

Applications of such location awareness could be signal acquisition and tracking, or they can be used to determine the need for high sensitivity receivers. For example, an increased integration time can be used if the estimated CNR falls below a certain threshold (e.g., of 20dB/Hz, as discussed in Section 2). Naturally, this on-off information can be further employed for indoor location awareness and in the acquisition and tracking processes. For instance, we could set the coherent integration times to high values (e.g., few hundreds of ms) if the CNR identifier indicates that we are in an indoor environment, compared with the situation when we are in an outdoor scenario. Moreover, the concept of CNR estimation based on the LCR information is a completely new concept to the authors' knowledge. So far, the LCR curves have been traditionally used for determining the terminal speed and Doppler frequency estimation [2] or to characterize the average duration of fades of various wireless channels [5]. Therefore, our proposed solution offers new research challenges for further investigation.

The paper is organized in the following manner. Firstly, in Section 2 we present the background theory of the signal model. Then, in Section 3 we introduce the basic concept that the novel indoor/outdoor identifier is based on, as well as a detailed description of it. In Section 4 we report the simulation results and we interpret them. Finally, in Section 5 we draw the conclusions and we present our suggestions for future open research issues.

---

\*This work was carried out in the project "Advanced Techniques for Personal Navigation" (ATENA) funded by the Finnish Funding Agency for Technology and Innovation (Tekes). This work has also been supported by the Academy of Finland.

## 2. SIGNAL MODEL

The signals of interest here are GPS and Galileo civil signals. Both use a Direct-Sequence Code Division Multiple Access (DS-CDMA) technique, and either Binary Phase Shift Keying (BPSK), for C/A code of GPS, or sine Binary-Offset-Carrier (BOC) modulation, for Galileo Open Services [6, 7]. Therefore, the transmitted signal  $x(t)$  can be written as the convolution between the modulating waveform  $s_{BOC}(t)$ , the pseudorandom (PRN) CDMA code, including data modulation, and the pulse shaping filter  $p_{T_B}(t)$  [8]:

$$x(t) = \sqrt{E_b} s_{BOC}(t) \otimes \sum_{n=-\infty}^{+\infty} \sum_{k=1}^{S_F} b_n c_{k,n} \delta(t - nT_{sym} - kT_c) \otimes p_{T_B}(t) \quad (1)$$

where  $E_b$  is the data bit energy,  $\otimes$  is the convolution operator,  $b_n$  is the  $n$ -th complex data symbol (in case of a pilot channel, it is equal to 1),  $T_{sym}$  is the symbol period,  $c_{k,n}$  is the  $k$ -th chip corresponding to the  $n$ -th symbol,  $T_c = 1/f_c$  is the chip period,  $S_F$  is the spreading factor ( $S_F = T_{sym}/T_c$ ),  $\delta(t)$  is the Dirac pulse, and  $p_{T_B}(t)$  is the pulse shaping filter applied to pulses of duration  $T_B = T_c/N_B$ . Here,  $N_B$  is a modulation-related parameter, also named as BOC-modulation order (this was detailed in [8]). For example, for the most encountered GNSS modulations, namely BPSK and sine-BOC(1,1) modulations, we have:  $N_B = 1$  and  $N_B = 2$ , respectively. For example, if infinite bandwidth is assumed,  $p_{T_B}(t)$  will be a rectangular pulse of unit amplitude if  $0 \leq t \leq T_B$  and 0 otherwise. Above,  $s_{BOC}(t)$  stands for both BPSK and sine BOC-modulated signals, and it can be expressed as in eq. (2) [8] (for cosine-BOC modulation, the detailed expression of  $s_{BOC}(t)$  is given in [8]):

$$\begin{aligned} s_{BOC}(t) &= \text{sign} \left( \sin \left( \frac{N_B \pi t}{T_c} \right) \right), \quad 0 \leq t \leq T_c \\ &= \sum_{i=0}^{N_B-1} (-1)^i \delta(t - iT_B) \end{aligned} \quad (2)$$

The signal  $x(t)$  is typically transmitted over a multipath static or fading channel, where all interference sources (except the multipaths) are lumped into a single additive Gaussian noise term  $\eta(t)$ :

$$r(t) = \sum_{l=1}^L \alpha_l x(t - \tau_l) e^{-j2\pi f_D t} + \eta(t), \quad (3)$$

where  $r(t)$  is the received signal,  $L$  is the number of channel paths,  $\alpha_l$  is the complex coefficient of the  $l$ -th path,  $\tau_l$  is the channel delay introduced by the  $l$ -th path,  $f_D$  is the Doppler shift introduced by the channel, and  $\eta(t)$  is the additive Gaussian noise of zero mean and double-sided power

spectral density  $N_0$ . Typically, the signal-to-noise ratios for GNSS signals are expressed with respect to the code epoch bandwidth  $B_w$ , namely  $B_w = 1$  kHz [6, 7], under the name of Carrier-to-Noise Ratio (CNR). The relationship between CNR and bit-energy-to-noise ratio is as follows:

$$CNR[dB/Hz] = \frac{E_b}{N_0} + 10 \log_{10}(B_w). \quad (4)$$

Sometimes, CNR is expressed in dBm, and the relationship with bit-energy-to-noise ratio becomes:

$$CNR[dBm] = \frac{E_b}{N_0} + 20 \log_{10}(B_w) + 10 \log_{10}(kT_0). \quad (5)$$

where,  $k$  is Boltzmann constant ( $k = 1.3806503 * 10^{-23}$  Joule/Kelvin) and  $T_0$  is the room temperature in Kelvin ( $T \approx 300$  K). That is,

$$CNR[dBm] \approx CNR[dB/Hz] - 174 \text{ dBm/Hz}. \quad (6)$$

As far as the border between indoor/outdoor environments is concerned, there are several authors in the scientific community who discussed about it. Particularly, in [9] the authors considered this border to be about  $-155$  dBm, or approximately equal to  $18 - 19$  dB/Hz. In [10] the indoor environment is characterized by CNR values less than  $20$  dB/Hz, while in [11] it is stated that the indoor acquisition requires successful signal detection at typically  $20$  dB/Hz CNR level. Based on the above references we chose as the indoor/outdoor border the level of  $20$  dB/Hz to be used in our research.

Both acquisition and delay tracking stages (i.e., code synchronization) are usually based on the code epoch-by-epoch correlation  $\mathcal{R}(\cdot)$  between the incoming signal and the reference  $x_{ref}(\cdot)$  modulated PRN code, with a certain candidate Doppler frequency  $\hat{f}_D$  and delay  $\hat{\tau}$ :

$$\mathcal{R}(\hat{\tau}, \hat{f}_D, m) = \mathbf{E} \left( \frac{1}{T_{symp}} \int_{(m-1)T_{symp}}^{mT_{symp}} r(t) x_{ref}(\hat{\tau}, \hat{f}_D) dt \right), \quad (7)$$

where  $m$  is the code epoch index and  $\mathbf{E}(\cdot)$  is the expectation operation, with respect to the PRN code, and

$$x_{ref}(\hat{\tau}, \hat{f}_D) = \left( s_{BOC}(t) \otimes \sum_{n=-\infty}^{+\infty} \sum_{k=1}^{S_F} \hat{b}_n c_{k,n} \delta(t - nT_{sym} - kT_c) \otimes p_{T_B}(t) \right) e^{+j2\pi \hat{f}_D t} \quad (8)$$

where  $\hat{b}_n$  are the estimated data bits. For Galileo signals, a separate pilot channel is transmitted, thus the data bits are known at the receiver [7]. In order to reduce the noise level, both coherent and non-coherent integration are typically used. The averaged non-coherent correlation function

$\overline{\mathcal{R}}(\hat{\tau}, \hat{f}_D)$  can be written as:

$$\overline{\mathcal{R}}(\hat{\tau}, \hat{f}_D) = \frac{1}{N_{nc}} \sum_{N_{nc}} \left| \frac{1}{N_c} \sum_{m=1}^{N_c} \mathcal{R}(\hat{\tau}, \hat{f}_D, m) \right|^2 \quad (9)$$

where  $N_c$  is the coherent integration time (expressed in code epochs or ms for GPS/Galileo signals) and  $N_{nc}$  is the non-coherent integration time, expressed in blocks of length  $N_c$  ms.

If we assume that pilot channels are available or, equivalently, that data bits are perfectly estimated ( $\hat{b}_n = b_n$ ), that the random processes (i.e., noise, PRN codes, etc) are ergodic, and that the PRN codes have ideal correlations (i.e.,  $\mathbf{E}(c_{k,n}c_{m,p}) = 1$  if  $m = k$  and  $n = p$ , and  $\mathbf{E}(c_{k,n}c_{m,p}) = 0$  if  $m \neq k$  or  $n \neq p$ ), by replacing eqs. (1), (2), (3), (7), and (8) into eq. (9), we get, after several manipulations, that:

$$\overline{\mathcal{R}}(\hat{\tau}, \hat{f}_D) = E_b \left| \sum_{l=1}^L \alpha_l \mathcal{R}_{BOC}(\hat{\tau} - \tau_l) \text{sinc}(\pi \Delta f_D N_c T_{\text{symbol}}) \right|^2 + |\tilde{\eta}(\tau)|^2, \quad (10)$$

where  $\mathcal{R}_{BOC}(\cdot)$  is the auto-correlation of the BOC/BPSK modulation, including pulse shaping [8]:

$$\mathcal{R}_{BOC}(\tau) = \sum_{i_1=0}^{N_B-1} \sum_{i_2=0}^{N_B-1} (-1)^{i_1+i_2} \mathcal{R}_{\text{pulse}}(\tau - iT_B + i_1T_B), \quad (11)$$

$\mathcal{R}_{\text{pulse}}(\tau) = p_{T_B}(\tau) \otimes p_{T_B}(\tau)$  is the pulse shaping autocorrelation function (e.g., for rectangular pulses,  $\mathcal{R}_{\text{pulse}, T_B}(\tau)$  is a triangle of unit amplitude and support  $[-T_B, T_B]$ ),  $\Delta f_D = f_D - \hat{f}_D$  is the residual Doppler error, and  $\tilde{\eta}(\tau)$  is the filtered (coloured) noise of power spectral density  $N_0 \Pi(\frac{f N_c}{2B_w})$ , with  $\Pi(\cdot)$  is the rectangular pulse of unit amplitude and unit support. Above,  $\text{sinc}(x) = \sin(x)/x$ . Examples of the averaged correlation function of eq. (10), for BPSK and sine-BOC(1,1) modulation, one and two in-phase path channels, no noise, zero residual Doppler error and unit bit energy are shown in Fig. 1.

### 3. ANALYSIS OF NOVEL INDOOR/OUTDOOR IDENTIFIER

In this section we present the conceptual basis of the novel indoor/outdoor identifier, as well as a step-by-step description of its characteristics. As it was mentioned in Section 1, the basic idea behind the proposed identifier lies in making use of the LCR of the non-coherent averaged correlation function. The LCR at a certain level  $a$  is computed as the number of crossings (both from below and from above) of level  $a$ . Assuming that the time samples of the normalized correlation function  $\overline{\mathcal{R}}(\tau, f_D) / \max(\overline{\mathcal{R}}(\tau, f_D))$ , with  $\overline{\mathcal{R}}(\tau, f_D)$  given in eq. (10) are denoted by  $\overline{\mathcal{R}}_i$  and that they

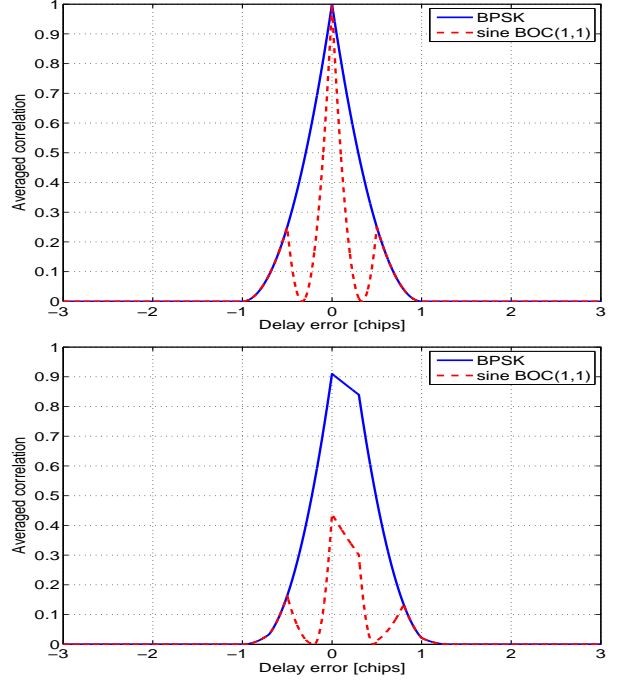


**Fig. 1.** Examples of averaged correlation function for BPSK and sine-BOC(1,1) modulation. Upper plot: single-path. Lower plot: two in-phase static paths, spaced at 0.3 chip distance; second path is 1 dB lower than the first.

are taken at sampling instants  $\tau_i, i = 1, 2, \dots$ , then:

$$LCR(a) = \text{card} \left\{ i | (\overline{\mathcal{R}}_i \leq a \wedge \overline{\mathcal{R}}_{i+1} > a) \wedge (\overline{\mathcal{R}}_{i+1} \leq a \wedge \overline{\mathcal{R}}_i > a) \right\}, \quad (12)$$

where  $\text{card}$  is the cardinal of a set and  $\wedge$  is 'and' operator. Additional insight on this can be gained from Fig. 2, where the Acf of the received sine BOC(1,1)-modulated signal is drawn, together with the LCR at level  $a = 0.2$  (here,  $LCR(0.2) = 4$ ). The channel in Fig. 2 is single-path static, where CNR is set to 30dB/Hz, the oversampling factor  $N_s$  (i.e., the number of samples per BOC interval) is equal to 10 and the values for non-coherent ( $N_{nc}$ ) and coherent ( $N_c$ ) integration are 2 and 20, respectively.

We define the AcfLevel as a vector  $[0.01 : 0.01 : 1]$  which divides the Acf in equally spaced stripes of 0.01 width (or resolution). In Fig. 2 these levels are represented with the parallel to the times axis, green dashed lines (for better readability, only the range  $[0.01 : 0.01 : 0.1]$  was depicted with its real resolution).

Based on Fig. 2, an intuitive notice is that in lower Acf levels the total number of crossings is likely to be higher than in higher Acf levels, due to the noise impact. Having this initial observation in mind, the basic idea was to com-

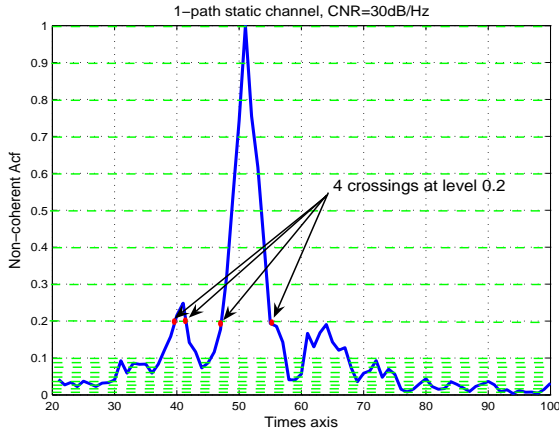


**Fig. 2.** Averaged LCR for 1-path static channel ( $N_{nc} = 2$ ,  $N_c = 20$ ).

pute the number of crossings for each value of the AcfLevel and examine how the Level Crossing Rate varies in terms of CNR. To implement this, we produced  $N_{rand} = 1000$  different random Acf realizations for each CNR value of the vector  $[10 : 5 : 40]$  dB/Hz and we computed the LCR for each realization. We used 1-path static channel, sampling rate  $N_s = 10$ , non-coherent integration length  $N_{nc} = 2$  blocks, and coherent integration length  $N_c = 20$  ms. Then, we computed the averaged LCR over  $N_{rand}$  and for each CNR. The averaged LCR information is depicted in Fig. 3 for CNR values 10 dB/Hz to 40 dB/Hz with step of 10.

From Fig. 3 we observe that there are certain characteristics of the LCR curve which are dependent on the CNR. These characteristics are: the number of maximum level crossings, the area below the LCR curve, and the position of the maximum level crossings in the AcfLevel. In particular, we notice that the maximum number of level crossings decreases from approximately 20 till 10 crossings as CNR increases from 10 to 40 dB/Hz. This variation, which is inversely proportional to the CNR, is also obvious in the case of the area which decreases when CNR increases. Lastly, in contrast with the previous two characteristics, the position of the maximum level crossings in the AcfLevel increases when we increase the CNR.

Based on the above mentioned observations, it became obvious that these three characteristics act as potential indoor/outdoor identifiers. The next step of our research was to examine thoroughly the behavior of the candidate identifiers in different channel profiles and search for the most reliable one. Based on extensive simulations, it became clear that the third characteristic, meaning the position  $\hat{a}$  of the maximum LCR in the AcfLevel, is the most promising:

$$\hat{a} = \arg \max_a LCR(a). \quad (13)$$

This identifier will be denoted from now on, as the “averaged Acf Level of max LCR”. Of course,  $\hat{a}$  is likely to vary according to the channel profile (static versus fading, single-path versus multipath). However, simulations showed that this variation is minor. For example, in Fig. 4 we show the variation of the averaged Acf Level of max LCR  $\hat{a}$  with CNR, for three channel profiles. The examined channels are: 1-path static, multipath static with randomly varying number of paths (uniformly distributed between 2 and 5), and multipath Nakagami-m fading channel with with randomly varying number of paths (uniformly distributed between 2 and 5) and a Nakagami-m factor equal to 0.65.

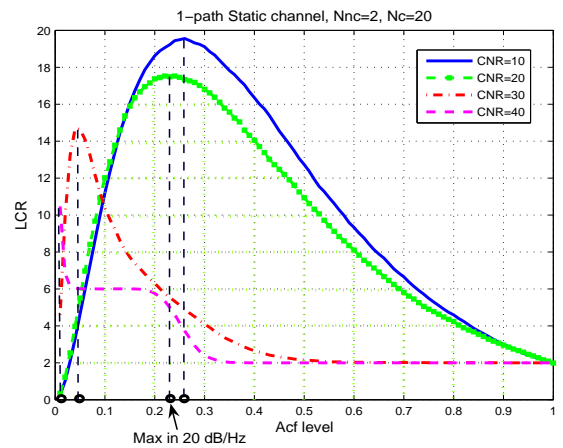


**Fig. 3.** Averaged LCR for 1-path Static channel ( $N_{nc} = 2$ ,  $N_c = 20$ ).

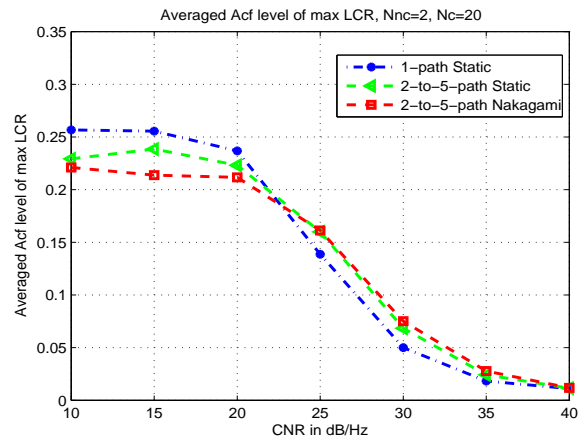


**Fig. 4.** Averaged Acf level for 3 channel profiles ( $N_{nc} = 2$ ,  $N_c = 20$ ).

From Fig. 4, it is clear that the difference among the three channel profiles is very small and therefore the Acf level of the maximum LCR has a great potential as a reli-

able CNR identifier, which is independent of the transmission channel. Before its performance is evaluated, we need to take into account the relationship of  $\hat{a}$  with the integration times, both coherent and non-coherent. This necessity comes from the fact that the CNR is higher after integration than before coherent and non-coherent integration, therefore this dependency needs to be taken into account. The CNR values given here are those of eq. (4), corresponding to 1 kHz bandwidth (i.e., before coherent and non-coherent integration). In Table 1 we present the averaged Acf level of max LCR versus  $N_{nc}$  and  $N_c$  for the fixed CNR value of 20 dB/Hz (we recall that this value was chosen as the border between the indoor and outdoor scenarios, as explained in Section 2). The averaging has been made over 1000 random Acf realizations and the channel is 1-path static.

**Table 1.** Averaged Acf level of the max LCR ( $\hat{a}$ ) versus  $N_{nc}$  and  $N_c$  for 1-path static channel and CNR=20 dB/Hz.

	$N_c = 10$	20	30	40	50
$N_{nc} = 2$	0.26	0.23	0.21	0.18	0.16
3	0.31	0.28	0.24	0.20	0.17
4	0.35	0.31	0.25	0.21	0.18
5	0.38	0.32	0.27	0.21	0.18
6	0.41	0.33	0.26	0.21	0.18

From the table we notice that the averaged Acf level increases when we increase the non-coherent integration time while it decreases when increasing the coherent integration time. We remark that we examined the  $N_{nc}/N_c$  influence for multipath static channel as well, and as expected from Fig. 4, the values were quite similar. Therefore, we can rely on the values from Table 1 in order to choose the indoor/outdoor threshold. The proposed algorithm has the following steps:

1. Compute the correlation function  $\overline{\mathcal{R}}(\tau, \hat{f}_D)$  between the incoming signal and the reference code (in base-band domain) at a certain estimated Doppler shift  $\hat{f}_D$  (given, for example, from the acquisition time) and for several time delays, within a certain window around the estimated coarse delay from the acquisition time. In our simulations, we used window lengths of 4 chips for single path channels and 8 chips for multipath channels. Normalize this correlation function via its maximum value and form the cost function  $J$ :  $J = \overline{\mathcal{R}}(\tau, \hat{f}_D) / \max(\overline{\mathcal{R}}(\tau, \hat{f}_D))$ .
2. Compute the instantaneous  $LCR(a)$  levels of  $J$ , for  $a = [0.01 : 0.01 : 1]$ .
3. Find out  $\hat{a}_{sim}$  (the averaged Acf Level of max LCR), based on the instantaneous (simulations-based) LCR.
4. If  $\hat{a}_{sim} \leq \hat{a}$  with  $\hat{a}$  given in Table 1, decide that we are in indoor scenario (i.e., that CNR is below 20

dB/Hz). If  $\hat{a}_{sim} > \hat{a}$ , decide that we are in outdoor scenario.

In the next section we present the simulation results and we discuss the performance of the novel indoor/outdoor identifier.

#### 4. SIMULATION RESULTS AND DISCUSSION

The target of our simulations was to evaluate the performance of the proposed indoor/outdoor identifier in different channel profiles. In particular, three channel profiles have been used: 1-path static, multipath static with number of paths uniformly distributed between 2 and 5, and Nakagami-m fading channel with Nakagami-m factor 0.65 and number of paths uniformly distributed between 2 and 5. The signal was sine BOC(1,1)-modulated, according to Galileo signal specifications [7], with oversampling factor,  $N_s$ , equal to 10. In addition, the CNR level varied from 10 to 40 dB/Hz, with a step of 5 dB/Hz and the channel first path delay was assumed to be uniformly distributed within the range  $[-0.05 \ 0.05]$  (for multipath channels, the separation between successive paths is also uniformly distributed between 0.05 and 0.3 chips, that is, we have closely-spaced paths). The performance measure is the success rate (in %) of correct indoor/outdoor distinction over the whole range of CNR values. Here we present the results for non-coherent integration times equal to 2 and 6.

Figs. 5 and 6 show the success rate of the indoor/outdoor identifier for  $N_{nc} = 2$  and  $N_{nc} = 6$ , respectively. We notice that the performance of the identifier increases when the values of  $N_{nc}$  and  $N_c$  increase, for all the three considered channel profiles. For  $N_{nc} = 2$ , the identifier has the best performance for the single-path static channel. The performance slightly degrades when multipath static channel is concerned, followed on by the performance in the multipath fading channel. For  $N_{nc} = 6$ , the relative performance among the channels varies with  $N_c$ . In particular, for low  $N_c$  ( $\leq 20$ ) the identifier performs the best for the single path static channel, while for higher  $N_c$  the identifier has the higher success rate for the multipath static channel. In both cases, we are able to achieve success rates up to 84% ( $N_{nc} = 2$ ) and 95% ( $N_{nc} = 6$ ) of cases.

In general, the identifier's capability for correct distinction between indoor and outdoor scenario varies from 67% to 84% for  $N_{nc} = 2$  and from 70% to 95% for  $N_{nc} = 6$ . In the worst case scenario, the identifier will predict correctly the indoor environment by 67% and its success level can be even up to 95%.

#### 5. CONCLUSIONS AND FUTURE WORK

Our paper introduces a CNR identifier based on the instantaneous level crossing rates of the correlation function be-

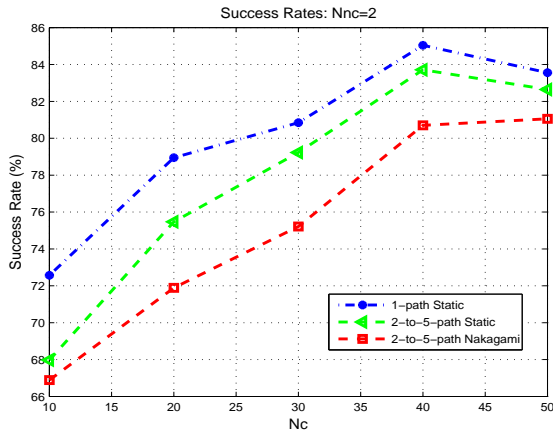


Fig. 5. Success Rates for  $N_{nc} = 2$ .

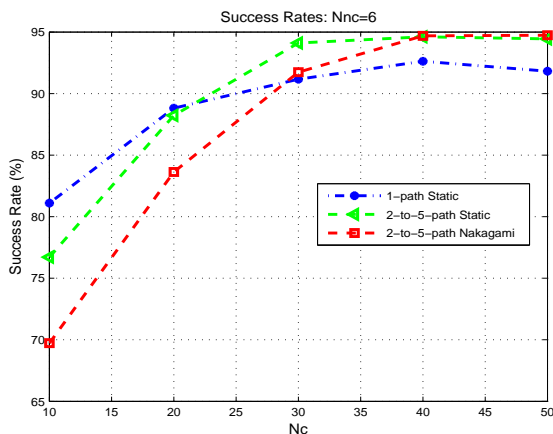


Fig. 6. Success Rates for  $N_{nc} = 6$ .

tween the incoming signal and the reference code. The purpose of such an identifier is to help the delay tracking process in GNSS systems, by furnishing some adaptive information according to the channel type, which can be used to adjust the integration times at the receiver. The implementational complexity is rather moderate, since the algorithm is based on the already existing correlation values (e.g., after the acquisition stage).

The simulations showed that the proposed identifier can reach prediction level up to 95% while retaining the success rate above 67% even in the worst case scenario. A natural continuation of our work would be to enhance the identifier's capability of indoor/outdoor distinction to a precise CNR estimator. One suggestion on this would be to have a set of CNR identifiers, their number of which would determine the desired precision of the estimation process. In other words, these identifiers would employ some threshold values derived for each CNR level from the correspond-

ing averaged LCR curve. Then, this set of identifiers would form a single CNR estimator. In addition, deeper research on the LCR concept may lead to the discovery of new characteristics (other than the position of the max LCR in the AcfLevel) that could act as reliable CNR identifiers.

## 6. REFERENCES

- [1] A. Schmid and A. Neubauer, "Carrier to Noise Power Estimation for Enhanced Sensitivity Galileo/GPS Receivers," in *IEEE*, 2005.
- [2] C. Tepedelenlioglu, A. Abdi, G. B. Giannakis, and M. Kaveh, "Estimation of doppler spread and signal strength in mobile communications with applications to handoff and adaptive transmission," *Wirel. Commun. Mob. Comput.*, 2001.
- [3] K. Ramasubramanian, "Performance Bounds for Carrier-to-Noise Ratio Estimation in GPS Receivers," in *ION NTM*, 2006.
- [4] M. Sayre, "A Block Processing Carrier to Noise Ratio Estimator for the Global Positioning System," in *ION NTM*, 2004.
- [5] G. Guerra, P. Angueira, M. Vélez, D. Guerra, G. Prieto, J. L. Ordiales, and A. Arrinda, "Field measurement based characterization of the wideband urban multipath channel for portable dtv reception in single frequency networks," *IEEE TRANSACTIONS ON BROADCASTING*, 2005.
- [6] E.D. Kaplan, *Understanding Gps: Principles and Applications*, Artech House, 1996.
- [7] "Galileo Joint Undertaking - Galileo Open Service, Signal in space interface control document (OS SIS ICD)," GJU webpages, <http://www.galileoju.com/> (active Oct 2006), May 2006.
- [8] E. S. Lohan, A. Lakhzouri, and M. Renfors, "Binary-Offset-Carrier modulation techniques with applications in satellite navigation systems," *Wiley Journal of Wireless Communications and Mobile Computing*, DOI: 10.1002/wcm.407, published on-line, Jul 2006.
- [9] F. van Diggelen, "Global Locate Indoor GPS Chipset and Services," in *ION GPS*, 2001.
- [10] P. Enge, "GPS Modernization: Capabilities of the New Civil Signals," in *Invited Paper for the Australian International Aerospace Congress*, 2003.
- [11] R. T. Ioannides and L. E. Aguado, "Coherent Integration of Future GNSS Signals," in *ION GNSS, 19th International Technical Meeting of the Satellite Division*, 2006.